

Phase diagram of nuclear matter created in relativistic nuclear collisions

V.A. Kizka¹

*V.N.Karazin Kharkiv National University,
4 Svobody Sq., 61022, Kharkiv, Ukraine*

Abstract. The published theoretical data of few models (PHSD/HSD both with and without chiral symmetry restoration) applied to experimental data from collisions of nuclei from SIS to LHC energies, have been analysed by using of the meta-analysis what allowed to localize a possible phase singularities of nuclear matter created in the central nucleus-nucleus collisions: The ignition of the Quark-Gluon Plasma's (QGP) drop begins already at top SIS/BEVALAC energies at around $\sqrt{s_{NN}} = 2$ GeV. This drop of QGP occupies small part, 15% (an averaged radius about 5.3 fm if radius of fireball is 10 fm), of the whole volume of a fireball created at top SIS energies. The drop of exotic matter goes through a split transition (separated boundaries of sharp (1-st order) crossover and chiral symmetry restoration (CSR) in chiral limit) between QGP and Quarkyonic matter at energy around $\sqrt{s_{NN}} = 3.5$ GeV. The boundary of transition between Quarkyonic and Hadronic matter with partial CSR was localized between $\sqrt{s_{NN}} = 4.4$ and 5.3 GeV and it is not being intersected by the phase trajectory of that drop. Critical endpoint of 2-nd order has been localized at around $\sqrt{s_{NN}} = 9.3$ GeV, a triple phase area appears at $12 \div 15$ GeV, a critical endpoint of 1-st order - at around $\sqrt{s_{NN}} = 20$ GeV, the boundary of smooth (2-nd order) crossover transition with CSR in chiral limit between Quarkyonic matter and QGP was localized between $\sqrt{s_{NN}} = 9.3$ and 12 GeV and between Hadronic and QGP on $\sqrt{s_{NN}} = 15$ and 20 GeV. The phase trajectory of a hadronic corona, enveloping the drop, stays always in the hadronic phase. A possible phase diagram of nuclear matter created in the mid-central nucleus-nucleus collisions are also presented in the same range of energies as for the central collisions.

Keywords: Quark-Gluon Plasma; Nucleus-nucleus collisions; QCD phase diagram.

1 INTRODUCTION

This work uses the meta-analysis (the analysis of analyses) of the published theoretical and experimental data. The meta-analysis extensively was used already in 18 – 19th centuries by Laplace [1] and astronomers [2] though this idea had been appeared even earlier among astronomers in 17th century and was developing further, especially after invention by Blaise Pascal the mathematical ways of dealing with the games of chance used for gambling. The procedure of projection of the results of the meta-analysis on a suitable phenomenology, in order to interpret the area of the worst description of the experimental data by theoretical models, is the procedure intruded in the presented analysis.

The main goal of this work is to figure out the possible phase diagram of strongly interacting matter using already available published material obtained during decades.

The work is organized as follows. In the next section, a simple form of the mathematical foundation of the meta-analysis is shown. Section 3 is devoted to the application of the obtained formulas to the published results from experimental and theoretical investigations in nucleus-nucleus collisions. Section 4 contains conclusion.

¹Valeriy.Kizka@karazin.ua

2 JUSTIFICATION OF THE METHOD

Let us consider some phenomenon P of an arbitrary nature. Let this phenomenon consist of several sub-processes: $P = \{p_1, p_2, \dots, p_y\}$. Let this phenomenon exist during a time interval and within some spatial volume $a_P = \{\tau_f(P) - \tau_0(P); V_f(P)\}$, and each sub-process also occupies own space-time interval: $a_{p_i} = \{\tau_f(p_i) - \tau_0(p_i); V_f(p_i)\}$, such that $a_{p_i} \in a_P, \forall i$. Let we observe a phenomenon P through measurements of some set of observables $B = \{B_1(\kappa_1), \dots, B_x(\kappa_x)\}$, where κ_i is a some variable. Each $B_i(\kappa_i)$ is responsible for several sub-processes which influence on $B_i(\kappa_i)$: $s(B_i(\kappa_i)) = \{p_m, \dots, p_r\} \subset P$, and $\bigcup_{i=1}^x s(B_i(\kappa_i)) = P$. And each sub-process p_i gives a contribution to several observables $s(p_i) = \{B_j(\kappa_j), \dots, B_t(\kappa_t)\} \subset B$, and $\bigcup_{i=1}^y s(p_i) = B$. In this case this set of observables B is called the complete set of observables - the sub-processes which influence on all observables of B form the set P .

Let experiment can measure any observable $B_i(\kappa_i) \in B$ within some interval of change of κ_i defined by an experimental conditions and this interval is broken into n_{B_i} bins $\kappa_i = \{\kappa_{i,1}, \dots, \kappa_{i,n_{B_i}}\}$ (number of data points): $B_i^{exp} = \{B_i^{exp}(\kappa_{i,1}), \dots, B_i^{exp}(\kappa_{i,n_{B_i}})\}$. A total set of measured observables is $B^{exp} = \{B_1^{exp}(\kappa_1), \dots, B_x^{exp}(\kappa_x)\} = \{B_1^{exp}(\kappa_{1,1}), \dots, B_1^{exp}(\kappa_{1,n_{B_1}}), \dots, B_x^{exp}(\kappa_{x,1}), \dots, B_x^{exp}(\kappa_{x,n_{B_x}})\}$. I consider each point of data on an equal basis with each other point as a separate observable.

Let us consider a set of the theoretical models $S(M) = \{M_1, \dots, M_s\}$ describing the considered phenomenon P . Each model M_i describes a phenomenon P , considering its consisting of a set of the sub-processes $P(M_i) = \{p_{1,i}, \dots, p_{w,i}\}$ defined within phenomenology of the model M_i . Note that the number of elements of sets P and $P(M_i)$ can be different. Let the model M_i allows to calculate the whole set of observables B , giving a set $B^{M_i} = \{B_1^{M_i}(\kappa_1), \dots, B_x^{M_i}(\kappa_x)\} = \{B_1^{M_i}(\kappa_{1,1}), \dots, B_x^{M_i}(\kappa_{x,n_{B_x}})\}$, where model M_i had been applied to each data point.

Let us introduce some function:

$$f_{M_k}(B_{i,j}) = f(B_i^{M_k}(\kappa_{i,j}), B_i^{exp}(\kappa_{i,j}), \sigma B_i^{M_k}(\kappa_{i,j}), \sigma B_i^{exp}(\kappa_{i,j})), \quad (1)$$

where $\sigma B_i^{exp(M_k)}(\kappa_{i,j})$ is an experimental(theoretical) error in j th point of $B_i^{exp(M_k)}(\kappa_i)$, and $f_{M_k}(B_{i,j}) \rightarrow 0$ if $B_i^{M_k}(\kappa_{i,j}) \rightarrow B_i^{exp}(\kappa_{i,j})$. This function f is a criterion of comparison of the model with an experiment in the given point.

Let us introduce the set according to (1) for all elements of sets B^{exp} and B^{M_k} : $f_{M_k}(B) = \{f_{M_k}(B_{1,1}), \dots, f_{M_k}(B_{x,n_{B_x}})\}$.

Now we need to recall the definition of a distance between two curves. Let two curves $y(x)$ and $y_1(x)$ are defined on the closed interval $x \in [a, b]$. Then distance between these two curves is a number $r > 0$: $r = \max|y_1(x) - y(x)|$ defined at $[a, b]$. In our application points of y_1 correspond to data points (elements) of $B_i^{exp}(\kappa_i)$ and points of y - to elements of $B_i^{M_k}(\kappa_i)$. The function f taken in the point which corresponds to distance between the model and an experiment for observable $B_i(\kappa_i)$ is a worst criterion:

$$f_{M_k}(B_i)_{worst} = f(B_i^{M_k}(\kappa_{i,d_i}), B_i^{exp}(\kappa_{i,d_i}), \sigma B_i^{M_k}(\kappa_{i,d_i}), \sigma B_i^{exp}(\kappa_{i,d_i})), \quad (2)$$

where d_i th point such that $|B_i^{exp}(\kappa_{i,d_i}) - B_i^{M_k}(\kappa_{i,d_i})|$ is a maximal in a comparison to other points of $B_i^{exp(M_k)}(\kappa_i)$. And $f_{M_k}(B_i)_{worst} \rightarrow 0$ if $B_i^{M_k}(\kappa_{i,d_i}) \rightarrow B_i^{exp}(\kappa_{i,d_i})$.

Let us reduce the set $f_{M_k}(B)$ having kept only criteria corresponding to distances between $B_i^{exp}(\kappa_i)$ and $B_i^{M_k}(\kappa_i)$, $\forall i$: $f_{M_k}(B)_{worst} = \{f_{M_k}(B_1)_{worst}, \dots, f_{M_k}(B_x)_{worst}\} \subset f_{M_k}(B)$. Now number of elements of $f_{M_k}(B)_{worst}$ equal to the number of elements of B : $n(f_{M_k}(B)_{worst}) = n(B) \equiv x$. If $B_i^{exp}(\kappa_i)$ contains only one point then it keeps in the analysis in any case. Thus, for each $B_i(\kappa_i)$ we have one number $f_{M_k}(B_i)_{worst}$.

Thus we have reduced the sets B^{exp} and B^{M_k} to $B_{worst}^{exp} = \{B_1^{exp}(\kappa_{1,d_1}), \dots, B_x^{exp}(\kappa_{x,d_x})\} \subset B^{exp}$ and $B_{worst}^{M_k} = \{B_1^{M_k}(\kappa_{1,d_1}), \dots, B_x^{M_k}(\kappa_{x,d_x})\} \subset B^{M_k}$, and $n(B_{worst}^{exp}) = n(B_{worst}^{M_k}) = n(B) \equiv x$. Here, again remind, d_i th point corresponds to where we have distance between $B_i^{exp}(\kappa_i)$ and $B_i^{M_k}(\kappa_i)$. Thus we might say that for each observable as for the function with some number of points we kept only one point where model M_k has the worst description of experiment because the used model does not incorporate some sub-process (or sub-processes), or model wrongly includes its.

It sounds very confusing that we keep only few data points for analysis, having thrown out the majority of them. But we need to recall that we use the complete set of observables defined in the beginning. That is, the union of sets of sub-processes to which the observables from B_{worst}^{exp} are responsible (which influence on them) is a set which, at least, is very close to the set P , thereby forming the phenomenon investigated: $\bigcup_{i=1}^{n(B)} s(B_i^{exp}(\kappa_{i,d_i})) = s(B_{worst}^{exp}) \subseteq \bigcup_{i=1}^{n(B)} s(B_i(\kappa_i)) = P$.

Constructing the same expression for some model M_k which considers the phenomenon P consisting of the set of sub-processes some of which do not exist in the phenomenon, thus $\{p_{1,k}, \dots, p_{w,k}\} \neq P$, gives $\bigcup_{i=1}^{n(B)} s(B_i^{M_k}(\kappa_{i,d_i})) = s(B_{worst}^{M_k}) \neq \bigcup_{i=1}^{n(B)} s(B_i(\kappa_i)) = P$. The use of the model $M_{\bar{k}}$ considering the phenomenon consisting of the set of sub-processes which all exist in P , thus $\{p_{1,\bar{k}}, \dots, p_{t,\bar{k}}\} \subseteq P$, gives $\bigcup_{i=1}^{n(B)} s(B_i^{M_{\bar{k}}}(\kappa_{i,d_i})) = s(B_{worst}^{M_{\bar{k}}}) \subseteq \bigcup_{i=1}^{n(B)} s(B_i(\kappa_i)) = P$. Here is possible the case that $w \neq t$ and both not equal to $n(P) (\equiv y)$ (number of elements of set P), then inevitably $t < y$.

Keeping for analysis all data points gives nothing new - the criteria of different models cover each other in the most interesting physical areas where some of the most interesting sub-processes are being suppressed by other ones, what distort the analysis, bringing us to a wrong conclusions [25]. This is the main idea of the presented analysis - to find the data points with the worst coincidence to applied theoretical models, which form again the complete set of observables or, at least, the set is a close to the complete. We insist that if you have 10 observables, forming the complete set of observables in your problem, each containing 100 data points then you may bravely throw out 990 points, having kept for the analysis only 10 points (the worst points) - one point per one observable, and, we again insist, you will not distort your analysis!

Now we can introduce the expression:

$$\Phi_{M_k}(B) = \frac{1}{n(B)} \cdot \sum_{i=1}^{n(B)} f_{M_k}(B_i)_{worst}, \quad (3)$$

which gives the averaged criterion of the model M_k which is equally spread over all area of the worst description of the experiment by this model. And $\Phi_{M_k}(B) \rightarrow 0$ if each $B_i^{M_k}(\kappa_{i,d_i}) \rightarrow B_i^{exp}(\kappa_{i,d_i}), \forall i$ (look at definition (2)). (In [25], this averaging was done with averaging over all data points of criteria (only χ^2), what hid the worst area, and next additional averaging was done between different models

containing incompatible content, what made analysis useless.) If we use two models M_k and $M_{\bar{k}}$ from above reasonings then inevitably $\Phi_{M_k}(B) > \Phi_{M_{\bar{k}}}(B)$.

Having repeated calculation (3) for all models of set $S(M)$ and knowing set $P(M_k) = \{p_{1,k}, \dots, p_{w,k}\}$ for all k we may figure out which model missed which sub-processes, which model wrongly used some of sub-processes comparing all $\Phi_{M_k}(B), \forall k$, with each other. But question is what if all of the models missed some sub-processes and there is not possibility to check them with existing level of mathematical methods?

The only way is to apply to the analysis some set of phenomenologies $F = \{F_1, \dots, F_l\}, l = n(F)$, each of which incorporates the missed sub-process/sub-processes together with considered in $S(M)$ (but still cannot apply their mathematical methods for comparison with experiment) what is possible if the minimal value from all obtained $\Phi_{M_k}(B), k \in [1, s], s \equiv n(S(M))$, far away from zero. Of course, this create some randomness in the finished result depending from taken phenomenologies F but this randomness might be maximally decreased if we take the best modern phenomenologies, though this choice has the element of individual taste.

Suppose each phenomenology F_i from F considers the phenomenon P consisting of the set of sub-processes $P_{F_i} = \{p_j, \dots, p_m\} \subseteq P$. When we obtained the sets of the worst criteria $f_{M_k}(B)_{worst}, \forall k$ with corresponding set of average criteria $\{\Phi_{M_1}(B), \dots, \Phi_{M_s}(B)\}, s \equiv n(S(M))$, the next step is to make the projection of set of these averaged criteria on the phenomenological picture created by F :

$$Proj : \{\Phi_{M_1}(B), \dots, \Phi_{M_s}(B)\} \longrightarrow \bigcup_{i=1}^{n(F)} P_{F_i}. \quad (4)$$

That is, we make a mapping from set of the worst averaged criteria of the used set of models on the set $\bigcup_{i=1}^{n(F)} P_{F_i}$. In principle, we need to consider the set of the worst averaged criteria $\{\Phi_{M_1}(B), \dots, \Phi_{M_s}(B)\}$ as union of two (or even more) sets each containing the worst averaged criteria calculated for the compatible models (models with not contradicting content).

Let we have h subsets of the compatible models $M^q = \{M_e, \dots, M_n\}_q \subset S(M), q \in [1, h], \bigcup_{q=1}^h M^q = S(M)$ and we know the sets of subprocesses used by each of those models inside q th subset $P^q(M_j) = \{p_{1,j}, \dots, p_{w,j}\}, j \in [e, n]$. Then projection (4) is equivalent to other projection $\bigcup_{q=1}^h (\bigcup_{j=e}^n s(B_{worst}^{M_j}))_q \longrightarrow (\bigcup_{i=1}^{n(F)} P_{F_i})$, where $(\bigcup_{j=1}^n s(B_{worst}^{M_j}))_q \subseteq \bigcup_{j=e}^n P^q(M_j)$. The main task is to find the i th set of compatible models which is maximally close to P : $(\bigcup_{j=e}^n s(B_{worst}^{M_j}))_i \longrightarrow (\bigcup_{i=1}^{n(F)} P_{F_i}) \subseteq P$, visible over minimum of the value $\Phi_{M^q=i} = \Phi_{M_e}(B) \otimes \dots \otimes \Phi_{M_n}(B) \equiv \frac{1}{n(M^q=i)} \sum_{j=e}^n \Phi_{M_j}(B)$ in comparison with other sets of compatible models, and with use of the set F (with use of $\bigcup_{i=1}^{n(F)} P_{F_i}$) to build the most possible picture of phenomenon.

In final, the formula (4) may be rewritten:

$$Proj : \{\Phi_{M^1}, \dots, \Phi_{M^h}\} \longrightarrow \bigcup_{i=1}^{n(F)} P_{F_i}. \quad (5)$$

As each phenomenology F_i from F cannot calculate the observables because of mathematical predicaments, they have deal with some physical parameters derived from set P_{F_i} . Therefore projection (5) is assumed to be done on the set of physical parameters. The possibility of correlation of criteria with the parameters of a physical system is shown for the relative criteria in the next section.

Let some subprocess $p_\varepsilon \in P$ happens in a negligible space-time interval $a_{p_\varepsilon} = \{\tau_f(p_\varepsilon) - \tau_0(p_\varepsilon); V_f(p_\varepsilon)\}$, which is a tiny in the comparison with space-time interval of the phenomenon P and all other subprocesses from P : $a_{p_\varepsilon} \ll a_P, a_{p_\varepsilon} \ll a_{p_i}, \forall i \neq \varepsilon$. Let this subprocess gives a contribution into the measured observables from set $s^{exp}(a_\varepsilon) = \{B_\beta^{exp}(\kappa_\beta), \dots, B_\mu^{exp}(\kappa_\mu)\} \subset B$. Each $B_i^{exp}(\kappa_i) \in s^{exp}(a_\varepsilon)$ is influenced by several subprocesses from set $s(B_i^{exp}(\kappa_i)) = \{p_m, \dots, p_r\} \subset P$. At first sight, this is impossible to distinguish subprocess p_ε since it is suppressed by a contribution from other subprocesses. Now we should take into account that for an experimental observable $B_i^{exp}(\kappa_i) \in s^{exp}(a_\varepsilon)$ there is a set of measurements for all n_{B_i} data points: $B_i^{exp}(\kappa_i) = \{B_i^{exp}(\kappa_{i,1}) \pm \sigma^{exp}(B_i(\kappa_{i,1})), \dots, B_i^{exp}(\kappa_{i,n_{B_i}}) \pm \sigma^{exp}(B_i^{exp}(\kappa_{i,n_{B_i}}))\}$. Let's introduce a hypothesis H .

H : Among all observables from $s^{exp}(a_\varepsilon) \subset B$ there is at least one, $B_i^{exp}(\kappa_i), i \in [\beta, \mu]$, which has at least one such g th point of data, $B_i^{exp}(\kappa_{i,g}) \pm \sigma^{exp}(B_i(\kappa_{i,g}))$, which is influenced by subprocess p_ε in the not small degree at least comparable to the influences of other subprocesses. I.e., in a very narrow area of measurements corresponding to this g th point of data, subprocess p_ε gives a largest contribution in the comparison to its influences in the other data points.

Let there is a set of mutually compatible models $M(\bar{p}_\varepsilon) \in S(M)$ each of which does not assume existence of the subprocess p_ε in the phenomenon P . According to hypothesis H each of these theories should have the maximal difference between theoretically calculated and measured observable in g th point of data of $B_i^{exp}(\kappa_{i,g})$ in comparison with distances for other data points. If we use only one point of data of each observable, where difference between model and measurements is largest, we artificially separate the area with, probably, the largest manifestation of the p_ε . Having calculated and averaged criteria calculated for such points over all observables and having combined all compatible models, the obtained criteria $\Phi_{M_1(\bar{p}_\varepsilon) \otimes \dots \otimes M_e(\bar{p}_\varepsilon)}(B), M_i \in M(\bar{p}_\varepsilon), i \in [1, e]$, should be maximal if p_ε appears in P .

Otherwise, for a set of mutually compatible models $M(p_\varepsilon) \in S(M)$ each of which assumes existence of subprocess p_ε in the phenomenon P the worst criterion $\Phi_{M_1(p_\varepsilon) \otimes \dots \otimes M_y(p_\varepsilon)}(B)$ should be less than $\Phi_{M_1(\bar{p}_\varepsilon) \otimes \dots \otimes M_e(\bar{p}_\varepsilon)}(B)$.

Let us make assumption that formula (3) does not work - the value calculated by its does not reflect degree of coincidence of the model with experiment because of especial properties of model (does not matter which properties - laws of symmetries/conservations and so on) - that value may be very large even for the excellent coincidence of the model with an experiment: $\Phi_{M_k}(B) \rightarrow M \gg 0, M \in \mathbf{R}$, if each $B_i^{M_k}(\kappa_{i,d_i}) \rightarrow B_i^{exp}(\kappa_{i,d_i}), \forall i$. This is meaning that $\Phi_{M_k}(B)$ depends from some parameter λ_k which characterizes (reflects) those especial properties of particular model M_k : $\Phi_{M_k}(B, \lambda_k)$. But obtained new function violates our definition of averaged criterion given in (3) because these are two absolutely different functions. Therefore our supposition concerning of an existence of models with especial properties is wrong.

Imagine an object O , one part of which O_1 we can observe, and the other part O_2 we cannot observe, and even imagine in general, and $O = O_1 \cup O_2; O_1 \cap O_2 = \emptyset$. According with Kant's definition of the phenomenon as "the sensible concept of an object" [3], any phenomenon can be expressed as a set of sub-processes which are understandable completely by human brain with inherited to us on

birth the senses of time and of space [4], [7], i.e. the phenomenon (O_1) can be investigated by the experimentally-mathematical (scientific) methods (which strongly rely on the space and time notions), and this cognition of an object is possible up to the some limit - up to a noumenon $\partial O_2 \subset O_2$ which is a boundary of our understanding of an object [5]. Then $O_1 = \{p_1, p_2, \dots, p_y\} \equiv P$. Thus O_2 is a set (the exterior of set O_1) which cannot be understood with use of a space and time notions (i.e., it cannot be investigated by the experimentally-mathematical (scientific) methods) - object(thing) in itself [6]. O_2 is the insensible concept of an object O connected over noumenon ∂O_2 to a phenomenon O_1 and which can be never understood by means of human brain. Thus each object O can be cognized up to some limit ∂O_2 behind which the rationality loses sense. As we observe the phenomenon O_1 over measuring the complete set of observables B what permit us to localize the phenomenon inside space-time interval of its existence a_P we may rewrite expression for an object $O = \{B^{exp}, \bar{B}^{exp}\}$, where \bar{B}^{exp} is now a set of anti-observables which cannot be measured in the space and time because the elements of \bar{B}^{exp} are influenced by a set O_2 associated with a thing in itself. Having kept for the analysis the reduced set of observables B_{worst}^{exp} we reduce the number of elements in the set O without losing its meaning $O \supseteq \{B_{worst}^{exp}, \bar{B}^{exp}\}$. Thus, we move the analysis maximally closer to a noumenon of the studied phenomenon, i.e. we make analysis staying on the very brink of our knowledges about phenomenon.

In the following analysis, we use a set of observables taken for central nuclear collisions, which is at least close to complete. A deviation from this rule was made for semi-central collisions of heavy ions, although since the construction of the QCD phase diagram for this case was largely based on the results obtained for central nuclear collisions, we believe that the picture is not distorted significantly.

Since this analysis involves the use of theoretical models already superimposed on the experimental data, the procedures with fitting different sets of parameters before applying the model to the experimental data have nothing to do with the presented method.

3 APPLICATION OF THE METHOD

In this work, I use the set of worst criteria $\{\Delta_{worst}, \delta_{worst}, \chi_{worst}^2\}$, where Δ_{worst} is a maximal absolute deviation, δ_{worst} is the worst relative criterion and the last is the worst χ^2 -criterion. χ^2 -criterion and relative criterion were calculated only for that point of data of each observable where absolute deviation is maximal in comparison to all other points. Thus, I have excluded, in some degree, the dependence of χ^2 from experimental error, and relative criterion from relative scale, applying upon them restriction - take for analysis only criteria with maximal absolute deviations (see below).

Calculation of criteria was done by the next formulas:

$$\Delta_{worst}(B_i) = \max \left| B_i^{exp}(\kappa_{i,j}) - B_i^{th}(\kappa_{i,j}) \right|, j \in [1, n_{B_i}], \quad (6)$$

$$\delta_{worst}(B_i) = \left| \frac{\Delta_{worst}(B_i)}{B_i^{exp}(\kappa_{i,d_i})} \right| \pm \sigma(\delta_{worst}(B_i)), \quad (7)$$

$$\chi_{worst}^2(B_i) = \frac{(\Delta_{worst}(B_i))^2}{\sigma_{exp}^2(B_i(\kappa_{i,d_i}))} \pm \sigma(\chi_{worst}^2(B_i)), \quad (8)$$

where κ_i is a some of the variables shown below, $B_i(\kappa_{i,d_i})$ is a some d_i th data point of observable $B_i(\kappa_i)$, corresponding to the distance between theoretical and measured values: $|B_i^{exp}(\kappa_{i,d_i}) - B_i^{th}(\kappa_{i,d_i})| > |B_i^{exp}(\kappa_{i,j}) - B_i^{th}(\kappa_{i,j})|, \forall j \neq d_i$. $\sigma_{exp}(B_i(\kappa_{i,d_i}))$ is an experimental error for this d_i th point of data. If error $\sigma(\delta_{worst}(B_i)) > \delta_{worst}(B_i)$ (or $\sigma(\chi_{worst}^2(B_i)) > \chi_{worst}^2(B_i)$) then such criterion was thrown out from analysis to reduce a resultant error and other data point satisfying the above demands had been taken if it existed for given observable. (The reason of this is that we need to pull out the sub-processes which are negligibly influencing on the system but having crucial importance for understanding the evolution of fireball.) In result, statistics is different for different models and criteria.

The next set of models was used: $S(M) = \{ \text{HSD, PHSD, HSDwCSR, PHSDwCSR} \}$, where Hadron-String Dynamics without chiral symmetry restoration (HSD) transport approach applied to experimental data for central nucleus-nucleus ultra-relativistic collisions from SIS/BEVALAC to top RHIC energies was taken from [8],[9],[10],[11],[12],[13],[14],[15],[16],[17],[18], Parton-Hadron-String Dynamics without chiral symmetry restoration (PHSD) transport approach applied to experimental data for central nucleus-nucleus ultra-relativistic collisions from top SIS to LHC energies was taken from [8],[9],[12],[13],[18],[19],[20],[21],[22]; Hadron-String Dynamics with chiral symmetry restoration (HSDwCSR) transport approach applied to experimental data for central nucleus-nucleus ultra-relativistic collisions from AGS to SPS energies was taken from [18], Parton-Hadron-String Dynamics with chiral symmetry restoration (PHSDwCSR) transport approach - from [18]. PHSD differs from HSD by incorporation of the partonic degrees of freedom (QGP formation) in the dynamical processes. HSD and PHSD models has different versions in the used literature, but all versions were combined together (their averaged criteria, obtained by (3), were averaged also) because each next version does not contradict to preceding one, the new included sub-processes could be considered as mutually compatible to the other sub-processes.

The next set of observables taken from above mentioned articles was used in the analysis: the transverse mass $\kappa_1 = m_T$ or momentum $\kappa_2 = p_T$ (or total momentum $\kappa_3 = p$ only for BEVALAC/SIS energies) distributions of invariant yields $B_{1-3}(\kappa_{1-3}) = \frac{1}{(m_T, p_T)} \frac{d^2 N}{d(m_T, p_T) dy}(m_T, p_T)$, $E \frac{d^3 \sigma}{d^3 p}(p)$, the longitudinal rapidity $\kappa_4 = y$ distributions $B_4(\kappa_4) = \frac{dN}{dy}(y)$, the hadronic yields measured at midrapidity $B_5(\kappa_5) = \left. \frac{dN}{dy} \right|_{y=0}$, the total yields measured within 4π solid angle $B_6 = Y$ (one wide bin for rapidity) and dilepton invariant mass distributions $B_7(\kappa_7) = \frac{dN_{ll}}{dM_{ll}}(M_{ll})$. First six observables were taken for light flavor and strange hadrons, and $B_2(\kappa_2)$ was taken also for direct photons. The neutral transverse energy distribution for the opposed charged dimuons $\frac{dN}{dE_T}(E_T)$ is also used (only for $\sqrt{s_{NN}} = 17.3$ GeV). Calculation of the worst criteria was done separately for each type of particles (using (6)-(8)) and then their averaged values (obtained according with (3)) had been again averaged according with formulas at Fig. 1. The same formulas are used for the worst χ^2 -criteria at Fig. 2.

Taking into account reasonings (taking into account phenomenologies) from [18] (F_1), [23] (F_2) and [24] (F_3), interpretation of Fig. 1 and Fig. 2 is next. The separation of the worst χ^2 -criteria of PHSD and HSD models already at $\sqrt{s_{NN}} = 2.7$ GeV (they only touch each other by errors) could be caused by ignition of QGP at top SIS energies (the full star at Fig. 3). (Here the projection (5) of set of the worst averaged criteria $\{ \langle \chi^2(\text{HSD}) \rangle, \langle \chi^2(\text{PHSD}) \rangle, \langle \delta(\text{HSD}) \rangle, \langle \delta(\text{PHSD}) \rangle \}$ was done on the set $\{T, \mu_B\}$, formed by the set P_{F_3} , taken above of the line of deconfinement at large μ_B and finite T of Fig.5 of [24]. The correlation of criteria with parameters of system is shown below for relative criteria.) The next mapping goes also from results at Fig. 1 and Fig. 2 to the set $\{\mathbf{T}, \mu_{\mathbf{B}}\}$

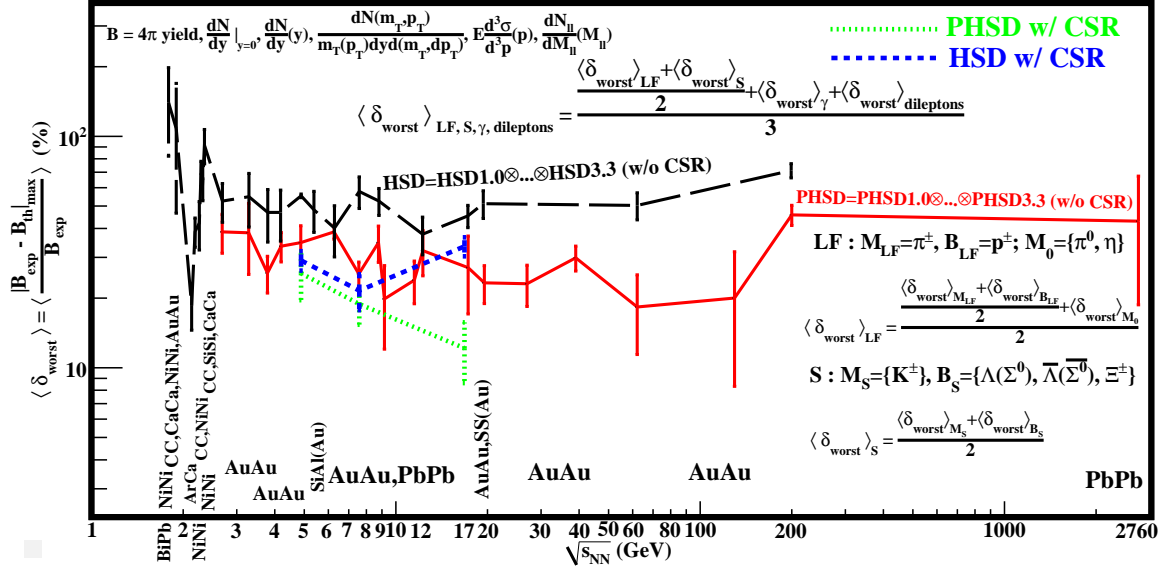


Figure 1: The worst relative criteria of comparison between models and experimental data as a function of the energy of central nucleus-nucleus collisions. The formulas are demonstrating the method described in the text. LF, S are a sets of light flavor and strange hadrons respectively. The symbol of tensor product is to show that used versions of models do not contradict to each other in contrast with [25] where, for example, the mix of 3FD with 1-st order phase transition and PHSD with crossover was made what is a nonsense. The points are connected by the lines to guide the eye.

depicted at Fig.5 of [24]. Remind that dependence of the worst χ^2 -criterion from an experimental error is reduced as described above. As partonic degree of freedom uses at most 40% of the collision energy at top SPS energies [23] then it would be possible to say that at top SIS energies this QGP state of matter should occupy small part of a volume of the created fireball (other its largest part of volume consist of hadronic matter). Then the fireball can be regarded as consisting of a drop of the hot and dense exotic matter with temperature greater than temperature of the fireball's peripheral hadronic corona ($\bigcup_{i=1}^3 P_{F_i}$). The separation of the worst relative criteria of PHSD and HSD models at around $\sqrt{s_{NN}} = 3.5$ GeV could be explained by the transition of QGP phase into Quarkyonic phase of matter - phase trajectory of a system (of a drop of exotic matter) intersect phase boundary (the point 3.5 GeV at Fig. 3). (Because of imposing of χ^2 for both models I admit, despite the separation of relative criteria, the crossing of the line of deconfinement by phase trajectory of a drop at this energy. Thus we make projection of set of worst criteria on the set of temperature and baryochemical potential on line of deconfinement at Pic.5 of [24].) The phase trajectory of hadronic corona stays in the hadronic phase at this energy of collisions (Corona's trajectory up to the point 3.5 GeV at Fig. 3). The energy pumped up into the fireball during nuclei collision is not enough to support the QGP phase in the drop at $\sqrt{s_{NN}} = 3.5$ GeV because of increased volume of the fireball in comparison with its volume at top SIS energies (the estimation of volume is shown below). The separations of the worst relative criteria on interval $\sqrt{s_{NN}} = 4.3$ GeV - 5.2 GeV and the worst χ^2 -criteria of PHSD and HSD models on interval $\sqrt{s_{NN}} = 4.6$ GeV - 5.5 GeV give hint that at energy around $\sqrt{s_{NN}} = (4.3+4.6)/2 = 4.45$ GeV the phase trajectory of a drop reaches the boundary between Hadronic and Quarkyonic states of matter (the point 4.4 GeV at Fig. 3). (I admit that temperature should be constant during phase transition and looking at Fig.5 of [24] we inevitably hit against the mentioned boundary.) That is, the pumped up energy into the fireball at $\sqrt{s_{NN}} = 4.4$ GeV is not enough to support Quarkyonic phase of matter of a drop because of, again, the increased volume of the fireball. The phase trajectory does not intersect this boundary but goes along it (the matter stays in the pre-Quarkyonic phase which is a some kind of confined matter which is different from pure hadronic one [26], and for such supposition I take into account the large values of both types of the worst criteria for HSD/PHSD models at that energy interval. I admit next phenomenology F_4 from [26] but with changes ($\bigcup_{i=1}^4 P_{F_i}$.) up to point corresponding to the energy around $\sqrt{s_{NN}} = (5.5 + 5.2)/2 = 5.35$ GeV (the point 5.3 GeV at Fig. 3). (Thus, we made projection of set of worst criteria on the set of T and μ_B are around the boundary between Hadronic and Quarkyonic matter at Fig.5 of [24].) Subsequent overturn of the worst χ^2 -criteria of HSD and PHSD relatively to each other and coincidence of the worst relative criteria of both models could be interpreted as returning phase trajectory of a drop into the Quarkyonic phase after $\sqrt{s_{NN}} = 5.35$ GeV. That is, the pumped up energy into the fireball is enough to return drop's matter in the Quarkyonic phase. (We are projecting the set of worst criteria, corresponding to energies above $\sqrt{s_{NN}} = 5.35$ GeV, on the set $\{T, \mu_B\}$ taken inside Quarkyonic phase close to Triple Point and line of deconfinement of Fig.5 of [24].) At point corresponding to around $\sqrt{s_{NN}} = 9.3$ GeV the phase trajectory reaches the critical end point moving on inside of the Quarkyonic phase [24] (there the position of critical end point inside Quarkyonic phase was considered and I admit of reaching it from inside the phase) - I take into account the sharp decreasing of the worst relative criterion and χ^2 -criterion of PHSD after 8.8 GeV with their local minimums at $\sqrt{s_{NN}} = 9.2$ GeV and divergence of the worst relative criteria for PHSDwCRS and HSDwCRS after 9.2 GeV (taking

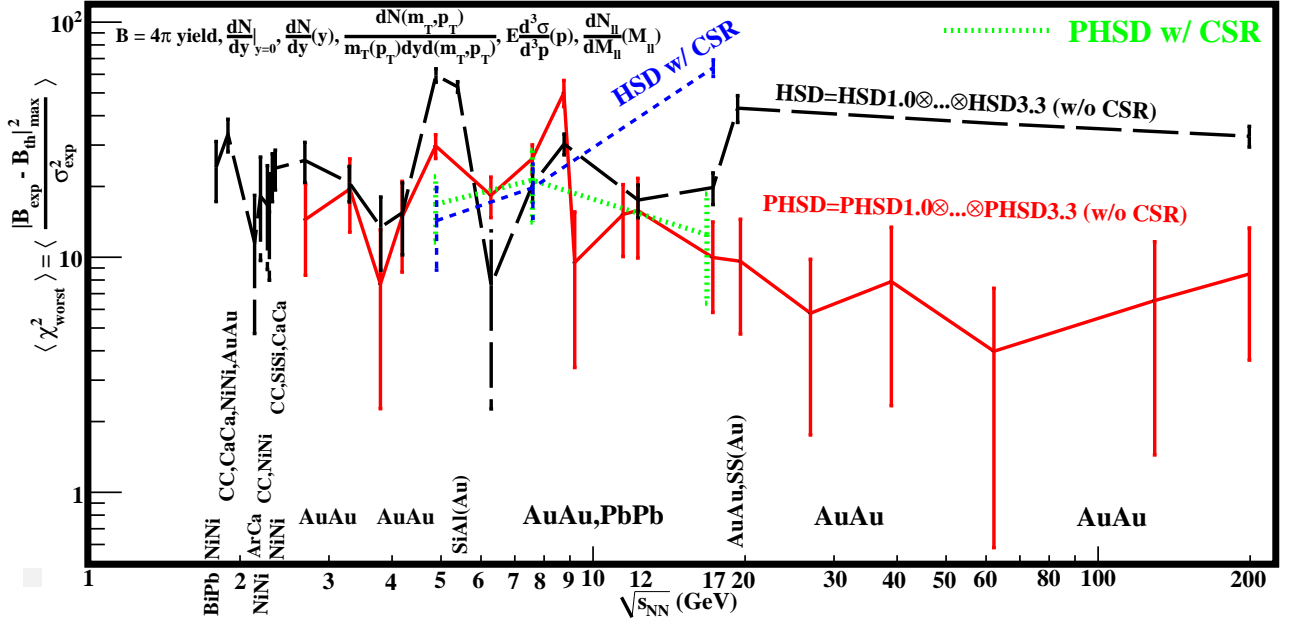


Figure 2: The worst χ^2 -criteria of comparison between models and experimental data as a function of the energy of central nucleus-nucleus collisions. The points are connected by the lines to guide the eye.

into account criteria' errors) and their the worst χ^2 -criteria after 10 GeV: $\frac{8.8+9.2+9.2+10}{4} = 9.3$ GeV. As PHSD assumes transition to QGP over smooth (2-nd order) crossover, the next similar behavior of two types of the worst criteria with their intersections at around $\sqrt{s_{NN}} = 12.3$ GeV I interpret as the subsequent moving of the phase trajectory of a drop, after critical end point, along boundary of transition with a smooth crossover between Quarkyonic and QGP phases up to Triple Point (Fig.5 of [24]). (Because both types of criteria for PHSD are increasing from the local extremums (local minimums) I admit the moving of phase trajectory of a drop in the QGP phase closely to a boundary up to the $\sqrt{s_{NN}} = 12.3$ GeV after which the trend is changing to a decreasing of PHSD criteria.) After Triple Point corresponding to around $\sqrt{s_{NN}} = 12.3$ GeV (the intersection is visible there for both types of criteria; the projection of set of criteria at $\sqrt{s_{NN}} = 12.3$ GeV on the set $\{T, \mu_B\}$ at Triple Point on Fig.5 of [24]) phase trajectory of a drop remains in the QGP phase. The phase trajectory of corona's matter stays in the hadronic phase at all range of considered energies of nuclear collisions. At the Fig. 3, a possible scenario of phase trajectory of a drop at low SIS/BEVALAC energies (dash dot line) was shown but other models (and phenomenologies) are needed to figure out that phase trajectory.

Temperature and baryon chemical potential at Fig. 3 are understood by me as a values averaged over all time of existence of drop or corona and over their volumes, but not as commonly used a freeze-out values [27]. That is, let the drop (corona) exist during time interval $\Delta_{d(c)} = \tau_f - \tau_0$, where τ_0 is a time of formation of a drop (corona) and τ_f is a time of disappearing of a drop (corona). The temperature of a drop is higher than corona and it increases toward center of a drop.

Moreover, it is a function of time. The averaged volume of a drop (corona) over time interval its existence is $V_{d(c)} = \frac{1}{\Delta_{d(c)}} \int_{\tau_0}^{\tau_f} V_{d(c)}(t) dt$. Then averaged temperature of a drop (corona) is $T \equiv \langle T \rangle_{d(c)} = \frac{1}{\Delta_{d(c)} \cdot V_{d(c)}} \int_{\tau_0}^{\tau_f} \int_v T_{d(c)}(t, \vec{r}) dt d^3 \vec{r}$, $\langle T \rangle_d > \langle T \rangle_c$. And I assume that $\langle T \rangle_d > \langle T \rangle_{fball}$, where the average temperature of whole fireball obtained analogously. The same for the baryon chemical potential: $\mu_B \equiv \langle \mu_B \rangle_{d(c)} = \frac{1}{\Delta_{d(c)} \cdot V_{d(c)}} \int_{\tau_0}^{\tau_f} \int_v \mu_{Bd(c)}(t, \vec{r}) dt d^3 \vec{r}$.

Let us now estimate the radius of a drop and volumes of a drop and corona created in the central collisions of nuclei. I assume further that shape of a drop in any time of its existence has an arbitrary topology. Let experiment measures the yield of particles created during time of fireball's existence and produced overall volume of fireball Y_{fball}^{exp} . Assume that the phase of the matter of a drop is A and the phase of the matter of a corona is B . Let model M_1 describes fireball evolution paying no attention to co-existence of phase B with A , assuming only phase's A existence. Then model M_1 predicts yield of particles from phase A : $Y_A^{M_1}$. Let now model M_2 describes fireball evolution paying no attention to co-existence of phase A with B , assuming only phase's B existence. Then model M_2 predicts yield of particles from phase B : $Y_B^{M_2}$. But experimental value Y_{fball}^{exp} equal to sum of yields of particles from both phases: $Y_{fball}^{exp} = Y_A + Y_B$ and those summands cannot be measured separately by experiment. Suppose that there are such numbers (there are such properties of created matter) $a_{1(2)}$ that $a_1 = Y_{fball}^{exp}/Y_A \approx V_{fball}/V_d$, $a_2 = Y_{fball}^{exp}/Y_B \approx V_{fball}/V_c$, where $V_{d,c,fball}$ are an averaged volumes of a drop, corona, fireball over their life time up to freeze-out. Then relative criterion $\delta = |(Y_{fball}^{exp} - Y_{A(B)}^{M_{1(2)}})/Y_{fball}^{exp}| = |1 - Y_{A(B)}^{M_{1(2)}}/Y_{fball}^{exp}| = |1 - Y_{A(B)}^{M_{1(2)}}/(a_{1(2)} Y_{A(B)})|$. Now let models $M_{1(2)}$ can be regarded as very good. I.e., although they can strongly deviate from experiment: $Y_{A(B)}^{M_{1(2)}} \neq Y_{fball}^{exp}$, but at least approximately $Y_{A(B)}^{M_{1(2)}} \approx Y_{A(B)}$. Therefore, $\delta \approx |1 - 1/a_{1(2)}| \approx |1 - \frac{V_{d(c)}}{V_{fball}}|$. Thus, the averaged relative criteria for yields over all type of particles give possibility to estimate averaged volume of different phases of the fireball. Exactly saying, the averaged relative criterion for yields of all type of particles shows an averaged volume which is not occupied by phase considered by used model. In [28] I used larger statistics for yields than in this work because did not exclude criteria with large errors, what smeared the picture, but in result Fig.1 of [28] shows not only the agreement of the model with an experiment, but and relative volume of HG (hadron gas) in the range from AGS to RHIC energies. For example, the average volume which is not occupied by HG (3FD, 3-Fluid Dynamic, with hadronic EoS model) in the fireball created in the central heavy ion collisions at $\sqrt{s_{NN}} = 63$ GeV is 100%, what means that at this energy QGP phase fills a whole volume of the fireball. At $\sqrt{s_{NN}} = 2.7$ GeV, all 3 versions of used model, HG version and two QGP versions of 3FD, have the averaged relative criteria around 15%. It is logically to assume that not occupied by HG (3FD with hadronic EoS does not assume coexistence of other phases) the averaged volume is 15%: $V_{HG} = 85\%$, then $V_{QGP} = 100 - 85 = 15\%$. If we take radius of fireball created at $\sqrt{s_{NN}} = 2.7$ GeV is 10 fm [29], then radius of a drop of QGP is around 5.3 fm. Analogously, the volume of exotic drop at $\sqrt{s_{NN}} = 3.2$ GeV (Fig.1 of [28]) is around 10% of whole volume of fireball, therefore the drop's radius is around 5.1 fm if radius of fireball has been increased up to, for example, 11 fm. That is, small volume of QGP's drop does not mean its small radius because of cubic dependence between them. Now, let's take density of QGP is 0.7 fm^{-3} [29], then averaged distance between partons is 0.55 fm. Taking reasonings (taking phenomenology) from [30] (F_5) that if germ of new phase, immersed in the other phase, has size (5.1 fm) between the mean interparticle distance (0.55 fm) and the system size (11 fm) then this is a mesoscopic system "with deconfinement being rather a sharp crossover"

(1-st order) [30]. So, at around $\sqrt{s_{NN}} = 3.5$ GeV the preferential transition is a sharp crossover and taking into account reasonings from [31] this sharp crossover transition is split from CSR transition. Their boundaries meet in critical endpoint at $\sqrt{s_{NN}} = 9.3$ GeV. According to [31] (F_6), this splitting is a small (it lays inside the limits of theoretical uncertainties) and temperature of CSR is higher than deconfinement, sharp crossover in our case, temperature ($\bigcup_{i=1}^6 P_{F_i}$).

Suppose that the relative criterion cannot be used for figuring out the properties of the system. Let criterion (relative, absolute deviation or any other) is a function of theoretical and experimental observables $f(B_\xi^M(\kappa), B_\xi^{exp}(\kappa))$. Let some parameter of the system $a(\lambda, B_\xi^{exp}(\kappa))$ depends from values one of which is experimentally observable $B_\xi^{exp}(\kappa)$ and other λ is a not experimentally observable value. Let model M cannot exactly describe $B_\xi^{exp}(\kappa)$ because of different reasons - difficult mathematical predicaments, absence of the knowledges about structure of a considered system and so on. Suppose that phenomenology, used in the M , might give possibility to simplify the system's structure regarding the value $B_\xi^M(\kappa)$ closely coincides with λ . Then $a \simeq a(B_\xi^M(\kappa), B_\xi^{exp}(\kappa))$. Next supposition that functional dependence from variables in f and a coincides make approximate equality between them: $f(B_\xi^M(\kappa), B_\xi^{exp}(\kappa)) \approx a(\lambda, B_\xi^{exp}(\kappa))$. Thus, the first supposition about impossibility is wrong.

Deep downfall of both types of criteria for HSD at around $\sqrt{s_{NN}} = 2$ GeV I interpret as deconfinement transition of a drop of exotic matter. The Figure 4 of [18] shows that at $\sqrt{s_{NN}} = 4.9$ GeV rapidity distribution of charged pions is better described by HSDwCSR (I now veer from criteria calculations, returning to the standard analysis on a naked eye), rapidity distribution of K^+ and protons - by both PHSDwCSR and HSDwCSR in equal manner, rapidity distribution of K^- - by both PHSDwCSR, HSDwCSR and PHSD in equal manner, and rapidity distribution of $\Lambda + \Sigma^0$ - by both PHSDwCSR and HSDwCSR in equal manner only for y around 0, and by HSD and PHSD in equal manner for $|y| \geq 0.4$, and all of them in equal manner at $|y| \simeq 0.3$. All these force me to conclude that around $\sqrt{s_{NN}} = 4.9$ GeV we have partially restored chiral symmetry, what means that chiral order parameter (with respect to the quark mass) begins decrease starting from boundary transition of hadronic matter to quarkyonic. And in addition to this, from Figure 7 of [18] we see better agreement of HSDwCSR and of PHSDwCSR with K^+/π^+ ratio at $\sqrt{s_{NN}} = 3.3$ and 3.8 GeV, and HSD and PHSD with $(\Lambda + \Sigma^0)/\pi^-$ ratio at $\sqrt{s_{NN}} = 3.3, 3.8$ and 4.2 GeV. Thus, we may assume that chiral order parameter gets zero (chiral limit) on the boundary of deconfinement at around $\sqrt{s_{NN}} = 2$ GeV, and after $\sqrt{s_{NN}} = 3.5$ GeV it begin increases after passing deconfinement boundary by phase trajectory of a drop, moving from QGP, with increase of energy of collisions up to around $\sqrt{s_{NN}} = 4.4$ GeV where it gets the pre-Quarkyonic matter.

The Figure 5 of [18] shows that at $\sqrt{s_{NN}} = 7.6$ GeV rapidity distribution of charged pions and proton (only one point) is better described by PHSDwCSR and HSDwCSR in equal manner, rapidity distribution of K^+ - by HSDwCSR, rapidity distribution of K^- - by PHSDwCSR, and rapidity distribution of $\Lambda + \Sigma^0$ - by both PHSDwCSR and HSDwCSR in equal manner for $|y| \leq 0.8$, and by HSD and PHSD in equal manner for $|y| \geq 1.2$, and by PHSDwCSR, HSD and PHSD in equal manner at $|y| \simeq 1$. Two last cases relate to not central rapidity region. All these force to conclude that at $\sqrt{s_{NN}} = 7.6$ GeV the phase trajectory of a drop came closely to a boundary where chiral order parameter gets a chiral limit. In addition to this, from Figure 7 of [18] we see better agreement of HSDwCSR with K^+/π^+ and $(\Lambda + \Sigma^0)/\pi^-$ ratios at $\sqrt{s_{NN}} = 7.6$ GeV.

The Figure 6 of [18] shows that at $\sqrt{s_{NN}} = 17.3$ GeV rapidity distributions for all particles are better described by PHSDwCSR and HSD in equal manner, what forces to conclusion that at

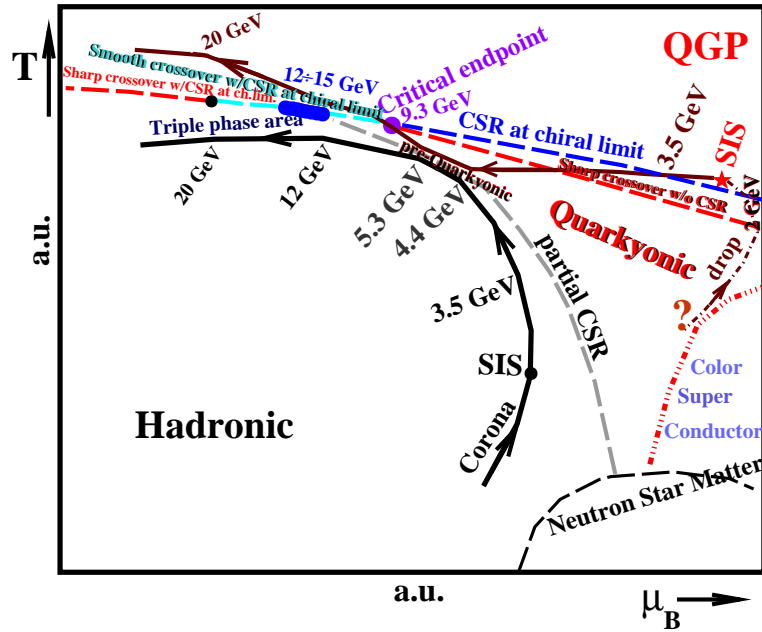


Figure 3: The sketch of the phase diagram of strongly interacting matter and the phase trajectories (with arrows) of a systems created in the central nucleus-nucleus collisions: Corona's phase trajectory - a phase trajectory of a matter of outer layer of a fireball; the drop's phase trajectory (solid with dash-dot line) - a phase trajectory of matter of central part of a fireball. Temperature T and baryon chemical potential μ_B are the values averaged over all time of existence and volume occupied by the drop or corona (see text).

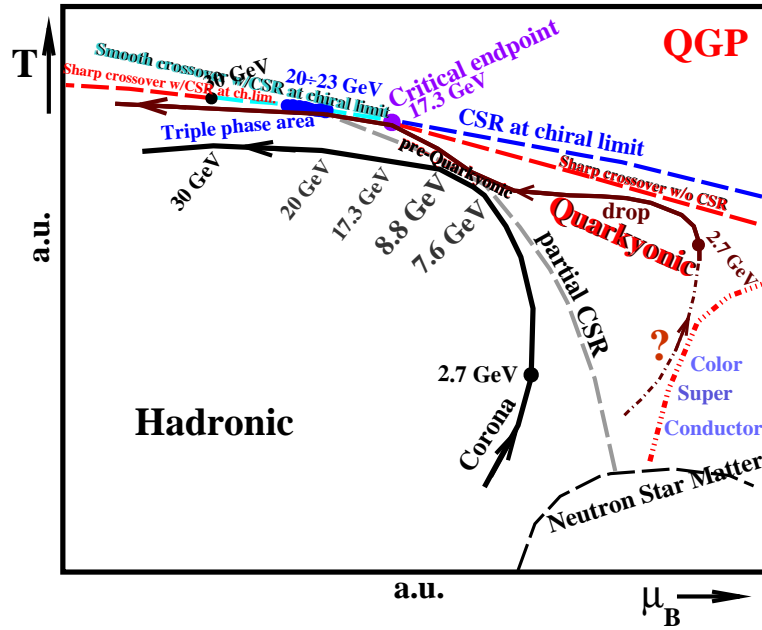


Figure 4: The same as for Fig. 3 but for the mid-central heavy-ion collisions. Temperature T and baryon chemical potential μ_B are the values averaged over initial space-time interval of existence of the drop or corona.

$\sqrt{s_{NN}} = 17.3$ GeV, though the phase trajectory of a drop is located in QGP phase, the state of matter of a drop is close to a hadronic phase on QCD phase diagram (the phase state of a drop is "feeling" the neighboring environment). This means that phase trajectory of a drop goes closely to a boundary of deconfinement transition (though I depict it on the Fig. 3 at larger distance for clarity of the picture). And in addition to this, from Figure 7 of [18] we see better agreement of HSD and PHSDwCSR with K^+/π^+ and $(\Lambda + \Sigma^0)/\pi^-$ ratios at $\sqrt{s_{NN}} = 17.3$ GeV.

I assume that area of triple point is prolonged from around $\sqrt{s_{NN}} = 12$ GeV to 15 GeV what explains close trend of both types of criteria for HSD and PHSD models between $\sqrt{s_{NN}} = 12$ and 17 GeV (in limit of errors). Therefore, the more conveniently to call it a triple phase area.

Parallel trend of both types of criteria for HSD and PHSD after $\sqrt{s_{NN}}$ around 20 GeV I interpret as existence some singularity around this energy. Relying on [32] (rapid crossover at high temperature and zeroth baryochemical potential - F_7) I should conclude that after $\sqrt{s_{NN}} = 20$ GeV (μ_B close to zero) there is a deconfinement boundary of the rapid crossover with, probably, CSR in chiral limit. That is we have the critical endpoint of first order at around $\sqrt{s_{NN}} = 20$ GeV. Relying on [33] I admit coincidence of CSR with deconfinement transition F_8 at μ_B close to zero ($\bigcup_{i=1}^8 P_{F_i}$).

Looking at Figure 2 of [28], we may immediately construct a QCD phase diagram of strongly interacting matter created in mid-central collisions of heavy ions ($\sqrt{s_{NN}} = 2.7 \div 27$ GeV), taking into account that used now observable, the directed flow of charged hadrons, sensitive to initial state of created matter [34], therefore this diagram is corresponding to non-equilibrated matter [35] (F_9)

(Fig. 4). I not assume reaching by phase trajectory of a drop to the deconfinement boundary at top SIS energies, during its initial time of existence, because both types of criteria for 3FD crossover EOS have large values starting from $\sqrt{s_{NN}} = 3.2$ GeV (note that here we have not the worst criteria but averaged over all data points of observable); before this energy it coincides with criteria for others EOS. The positions of singularities of matter are shifted to the higher energies of mid-central heavy-ion collisions in comparison to central ones. I assume that up to $\sqrt{s_{NN}}$ close to 30 GeV the phase trajectory of a drop does not enter in the QGP phase. Thus, I suggest existence in the hadronic phase the hadronic drop and with lower temperature the hadronic corona starting after around $\sqrt{s_{NN}} = 23$ GeV ($\bigcup_{i=1}^9 P_{F_i}$).

Thus, we have used the set of phenomenologies with nine elements $F = \{F_1, \dots, F_9\}$ each of which contains some assumptions, which are impossibility to check experimentally at present time. We can tell that we have made the mapping of the main phenomenology F_3 ([24]) by means of results of the meta-analysis, where the starting reference point of mapping has been taken in the point corresponding to $\sqrt{s_{NN}} = 2.7$ GeV, which we have placed in a QGP phase (for central nuclear collisions). And further we inserted all others phenomenologies $F \setminus F_3$ in the picture (in the Fig.5 of [24]) according with mapping, thereby forming a union $\bigcup_{i=1}^9 P_{F_i}$ of (5).

4 CONCLUSION

Application of the meta-analysis has allowed to separate HSD and PHSD models already at energy $\sqrt{s_{NN}} = 2.7$ GeV of central nucleus-nucleus collisions. The meta-analysis has figured out the possible position of a critical endpoint of second order at around $\sqrt{s_{NN}} = 9.3$ GeV, a critical endpoint of first order at around $\sqrt{s_{NN}} = 20$ GeV, a triple point at around $\sqrt{s_{NN}} = 12$ GeV (it probably occupy wide region, a triple phase area, on QCD phase diagram corresponding to around $\sqrt{s_{NN}} = 12 \div 15$ GeV) and the boundaries of a states of nuclear matter on QCD phase diagram: the transition at $\sqrt{s_{NN}} = 3.5$ GeV corresponds to a split sharp crossover (1-st order) transition and CSR in chiral limit (the last one at higher temperature, though this splitting lay in limit of theoretical uncertainties) between QGP and Quarkyonic matter, the boundary of transition with a partial CSR between Hadronic and Quarkyonic matter was localized between $\sqrt{s_{NN}} = 4.4$ and 5.3 GeV, though it is not being crossed by phase trajectories of a drop or corona. The boundary of a smooth crossover (2-nd order) transition with CSR in chiral limit between Quarkyonic matter and QGP was localized on interval $\sqrt{s_{NN}} = 9.3$ and 12 GeV, and between Hadronic matter and QGP on interval $\sqrt{s_{NN}} = 15$ and 20 GeV. After $\sqrt{s_{NN}} = 20$ GeV we have boundary of a sharp crossover transition with CSR in chiral limit between QGP and Hadronic matter.

The ignition of QGP's drop happens when phase trajectory of a drop goes through a split boundary transition of sharp crossover and CSR in chiral limit at around $\sqrt{s_{NN}} = 2$ GeV. The volume of this drop occupies about 15% of the total fireball volume.

Phase trajectory of a drop of matter of fireball created at mid-central heavy-ion collisions at energy range $\sqrt{s_{NN}} = 2.7 \div 27$ GeV do not reach the QGP state at these energies and during initial space-time interval of drop's evolution before getting an equilibrium state.

Other models are needed to figure out the phase trajectories of a system at lowest SIS and BEVALAC energies.

References

- [1] Laplace P-S. *Theorie Analytique des Probabilites. Oeuvres Completes* **7** (3rd edition). Paris: Courcier, 1820: lxxvii.
- [2] Airy G. B. *On the Algebraical and Numerical Theory of Errors of Observations and the Combination of Observations*. London: Macmillan and Company, 1861.
- [3] Immanuel Kant, *Critique of Pure Reason*. Cambridge University Press, 1998: p.276, "...phenomenon, or the sensible concept of an object,..."
- [4] Ibid: p.157, "...there are two pure forms of sensible intuition as principles of *a priori* cognition, namely space and time..."
Ibid: p.115, "In the analytical part of the critique it is proved that space and time are only forms of sensible intuition..."
- [5] Ibid: p.350, "The concept of a noumenon is therefore merely a boundary concept, in order to limit the pretension of sensibility..." Though Kant did not distinguish a noumenon from thing in itself, I admit his definition of noumenon as a boundary concept, keeping for thing in itself definition of Kant's successors (in addition to his in [6]): Stephen Palmquist, "Six Perspectives on the Object in Kant's Theory of Knowledge", *Dialectica* 40:2 (1986), pp.121-151: "...Thing-in-itself: an object considered transcendently apart from all the conditions under which a subject can gain knowledge of it via the physical senses. Hence the thing-in-itself is, by definition, unknowable via the physical senses. Sometimes used loosely as a synonym of noumenon..."
- [6] Ibid: p.421, "If matter were a thing in itself, then as a composite being it would be completely distinguished from the soul as a simple being. But it is merely an outer appearance, whose substratum is not cognized through any specifiable predicates;..."
Ibid: p.189, "Now through mere relations no thing in itself is cognized; it is therefore right to judge that since nothing is given to us through outer sense except mere representations of relation, outer sense can also contain in its representation only the relation of an object to the subject, and not that which is internal to the object in itself."
- [7] Tom J. Wills, Francesca Cacucci, Neil Burgess, John O'Keefe, "Development of the Hippocampal Cognitive Map in Preweanling Rats", *Science* **328**, Issue 5985, (2010) p. 1573-1576; DOI: <https://doi.org/10.1126/science.1188224>
Rosamund F. Langston *et al.*, "Development of the Spatial Representation System in the Rat", *Science* **328**, Issue 5985, (2010) p. 1576-1580; DOI: <https://doi.org/10.1126/science.1188210>
Linda Palmer, Gary Lynch, "A Kantian View of Space", *Science* **328**, Issue 5985, (2010) p. 1487-1488; DOI: <https://doi.org/10.1126/science.1191527>
- [8] W. Cassing *et al.*, "Parton/hadron dynamics in heavy-ion collisions at FAIR energies", Volume 95 (2015) EPJ Web of Conferences, 95 (2015) 01004; DOI: <https://doi.org/10.1051/epjconf/20159501004>; arXiv:1408.4313 [nucl-th].
- [9] W. Cassing, E.L. Bratkovskaya, "Parton-Hadron-String Dynamics: an off-shell transport approach for relativistic energies", *Nucl. Phys. A* **831**, (2009) 215-242; DOI: <https://doi.org/10.1016/j.nuclphysa.2009.09.007>; arXiv:0907.5331 [nucl-th].
- [10] J. Geiss, W. Cassing, C. Greiner, "Strangeness Production in the HSD Transport Approach from SIS to SPS energies", *Nucl. Phys. A* **644**, (1998) 107-138; DOI: [https://doi.org/10.1016/S0375-9474\(98\)80011-0](https://doi.org/10.1016/S0375-9474(98)80011-0); arXiv:nucl-th/9805012.

- [11] W. Cassing, E. L. Bratkovskaya, "Hadronic and electromagnetic probes of hot and dense nuclear matter", *Physics Reports* **308**, (1999) 65-233; DOI: [https://doi.org/10.1016/S0370-1573\(98\)00028-3](https://doi.org/10.1016/S0370-1573(98)00028-3).
- [12] E. L. Bratkovskaya *et al.*, "The QGP phase in relativistic heavy-ion collisions", Proceedings of the International Symposium on 'Exciting Physics', Makutsi-Range, South Africa, 13-20 November, 2011; DOI: 10.1007/978-3-319-00047-3_19; arXiv:1202.4891 [nucl-th].
- [13] E. L. Bratkovskaya *et al.*, "Properties of the partonic phase at RHIC within PHSD", 27th Winter Workshop on Nuclear Dynamics (WWND) in Colorado, USA on February 6 - 13, 2011; DOI: 10.1088/1742-6596/316/1/012027; arXiv:1106.1859 [nucl-th].
- [14] T. Anticic *et al.* (NA49 Collaboration), "System-size and centrality dependence of charged kaon and pion production in nucleus-nucleus collisions at 40 AGeV and 158 AGeV beam energy", *Phys. Rev. C* **86**, (2012) 054903; DOI: 10.1103/PhysRevC.86.054903; arXiv:1207.0348 [nucl-exp].
- [15] T. Anticic *et al.* (NA49 Collaboration), "System-size dependence of Lambda and Xi production in nucleus-nucleus collisions at 40A and 158 AGeV measured at the CERN Super Proton Synchrotron", *Phys. Rev. C* **80**, (2009) 034906; DOI: 10.1103/PhysRevC.80.034906; arXiv:0906.0469 [nucl-exp].
- [16] E. L. Bratkovskaya *et al.*, "Strangeness dynamics and transverse pressure in relativistic nucleus-nucleus collisions", *Phys. Rev. C* **69** (2004) 054907; DOI: 10.1103/PhysRevC.69.054907; arXiv:nucl-th/0402026
- [17] H. Weber, E. L. Bratkovskaya, W. Cassing, H. Stoecker, "Hadronic observables from SIS to SPS energies - anything strange with strangeness ?", *Phys. Rev. C* **67** (2003) 014904; DOI: 10.1103/PhysRevC.67.014904; arXiv:nucl-th/0209079
- [18] W. Cassing, A. Palmese, P. Moreau, E. L. Bratkovskaya, "Chiral symmetry restoration versus deconfinement in heavy-ion collisions at high baryon density", *Phys. Rev. C* **93**, (2016) 014902; DOI: 10.1103/PhysRevC.93.014902; arXiv:1510.04120v1 [nucl-th].
- [19] V. P. Konchakovski, W. Cassing, V. D. Toneev, "Impact of the initial size of spatial fluctuations on the collective flow in Pb-Pb collisions at $\sqrt{s_{NN}} = 2.76$ TeV", *J. Phys. G: Nucl. Part. Phys.* **42**, (2015) 055106; DOI: 10.1088/0954-3899/42/5/055106; arXiv:1411.5534 [nucl-th].
- [20] O. Linnyk *et al.*, "Hadronic and partonic sources of direct photons in relativistic heavy-ion collisions", *Phys. Rev. C* **92**, (2015) 054914; DOI: 10.1103/PhysRevC.92.054914; arXiv:1504.05699 [nucl-th].
- [21] Pierre Moreau *et al.*, "(Anti-)strangeness production in heavy-ion collisions", Proceedings of the 15th International Conference on Strangeness in Quark Matter (SQM2015), 6-11 July 2015, JINR, Dubna, Russia; DOI: 10.1088/1742-6596/668/1/012072; arXiv:1509.04455 [nucl-th].
- [22] E. L. Bratkovskaya *et al.*, "Dilepton production from SIS to LHC energies", Proceedings of the 28th Winter Workshop on Nuclear Dynamics, Dorado del Mar, Puerto Rico, April 7-14, 2012; DOI: 10.1088/1742-6596/389/1/012016; arXiv:1207.3198 [nucl-th].
- [23] O. Linnyk, E. L. Bratkovskaya, W. Cassing, "Strangeness production within Parton-Hadron-String Dynamics (PHSD)", *J. Phys. G: Nucl. Part. Phys.* **37**, (2010) 094039; DOI: 10.1088/0954-3899/37/9/094039; arXiv:1001.2914v1 [nucl-th].
- [24] A. Andronic *et al.*, "Hadron Production in Ultra-relativistic Nuclear Collisions: Quarkyonic Matter and a Triple Point in the Phase Diagram of QCD", *Nucl. Phys. A* **837**, (2010) 65-86; DOI: 10.1016/j.nuclphysa.2010.02.005; arXiv:0911.4806v3 [hep-ph].
- [25] V. A. Kizka, V. S. Trubnikov, K. A. Bugaev, D. R. Oliinychenko, "A possible evidence of the hadron-quark-gluon mixed phase formation in nuclear collisions", arXiv:1504.06483 [hep-ph].
- [26] Larry McLerran, Robert D. Pisarski, "Phases of Dense Quarks at Large N_c ", *Nucl. Phys. A* **796**, (2007) 83-100; DOI: 10.1016/j.nuclphysa.2007.08.013; arXiv:0706.2191v3 [hep-ph].

- [27] A. Bazavov *et al.*, "The curvature of the freeze-out line in heavy ion collisions", Phys. Rev. D **93**, (2016) 014512; DOI: 10.1103/PhysRevD.93.014512; arXiv:1509.05786v2 [hep-lat].
- [28] V. A. Kizka, "The comparison of the 3-fluid dynamic model with experimental data", arXiv:1508.03196 [nucl-th].
- [29] D. A. Fogaca, S. M. Sanches Jr., R. Fariello, F. S. Navarra, "Bubble dynamics and the quark-hadron phase transition in nuclear collisions", Phys. Rev. C **93**, 055204 (2016); DOI: 10.1103/PhysRevC.93.055204; arXiv:1601.04596v1 [hep-ph].
- [30] V.I. Yukalov, E.P. Yukalova, "Models of mixed hadron-quark-gluon matter", Proc. Sci. (ISHEPP) (2012) 046; arXiv:1301.6910 [hep-ph].
- [31] C. A. Dominguez, M. Loewe, Y. Zhang, "Chiral symmetry restoration and deconfinement in QCD at finite temperature", Phys. Rev. D **86**, (2012) 034030; DOI: 10.1103/PhysRevD.86.034030; arXiv:1205.3361v3 [hep-ph].
- [32] Y. Aoki *et al.*, "The order of the quantum chromodynamics transition predicted by the standard model of particle physics", Nature **443**, (2006) 675-678; DOI: 10.1038/nature05120; arXiv:0611014v1 [hep-lat].
- [33] S. Digal, E. Laermann, H. Satz, "Deconfinement through chiral transition in 2 flavour QCD", Nucl. Phys. Proc. Suppl. **94**, (2001) 389-392; DOI: 10.1016/S0920-5632(01)00982-3; arXiv:0010046 [hep-lat].
- [34] Yu.B. Ivanov, A.A. Soldatov, "Directed flow indicates a crossover deconfinement transition in relativistic nuclear collisions", Phys. Rev. C **91**, 024915 (2015); DOI: 10.1103/PhysRevC.91.024915; arXiv:1412.1669 [nucl-th].
- [35] L.V. Bravina *et al.*, "Equilibrium and non-equilibrium effects in relativistic heavy ion collisions", Nucl. Phys. A **661**, 600-603 (1999); DOI: [https://doi.org/10.1016/S0375-9474\(99\)85097-0](https://doi.org/10.1016/S0375-9474(99)85097-0).
S.A. Bass *et al.*, "Microscopic models for ultrarelativistic heavy ion collisions", Prog. Part. Nucl. Phys. **41**, 255-369 (1998); DOI: 10.1016/S0146-6410(98)00058-1.
M. Bleicher *et al.*, "Relativistic hadron-hadron collisions in the ultra-relativistic quantum molecular dynamics model", J. Phys. G **25**, 1859 (1999); DOI: <https://doi.org/10.1088/0954-3899/25/9/308>.